

Granular ‘glass’ transition

Leonardo E. Silbert¹, Deniz Ertaş², Gary S. Grest¹, Thomas C. Halsey², and Dov Levine³

¹ Sandia National Laboratories, Albuquerque, New Mexico 87185

² Corporate Strategic Research, ExxonMobil Research and Engineering, Annandale, New Jersey 08801

³ Department of Physics, Technion, Haifa, 32000 Israel

The transition from a flowing to a static state in a granular material is studied using large-scale, 3D particle simulations. Similar to glasses, this transition is manifested in the development of a plateau in the contact normal force distribution $P(f)$ at small forces, along with the splitting of the second peak in the pair correlation function $g(r)$, suggesting compaction and local ordering. The mechanical state changes from one dominated by plastic intergrain contacts in the flowing state to one dominated by elastic contacts in the static state. We define a staticity index that determines how close the system is to an isostatic state, and show that for our systems, the static state is not isostatic.

Granular materials are many-body systems which can exhibit properties of both liquids and solids, often at the same time. Features such as jamming in silos and hoppers [1] and heterogeneous force propagation [2] have motivated new proposals for constitutive relations for granular materials [3,4], in contrast to the established elasto-plastic theories [5,6]. Moreover, the emerging field of “jammed systems” [7] seeks to understand whether analogies may be drawn between diverse systems which have the common properties that they are far from equilibrium, and unable to explore phase space.

O’Hern *et al.* [8] have recently shown that similarities exist between the properties of *static* granular packings and other amorphous systems; in particular, they compared force distributions for simulated systems of soft-spheres undergoing a glass transition with experimental data from static granular packings [2,9]. These studies suggest that it may be interesting to consider the transition of granular materials from flowing to static, and inquire about its similarities with the glass transition. In this Letter we study the dynamic jamming transition of systems of athermal grains through large-scale simulation. In particular, we consider the behavior of dense packings of granular particles flowing down an inclined plane as the tilt angle θ is reduced through the angle of repose θ_r at which flow ceases.

The chute flow geometry we employ relies on gravity to compactify the system. Our earlier simulation studies in this geometry [10,11] have proven their reliability by reproducing key experimentally observed characteristics of dense granular flows [12], such as the existence of steady state flow over a range of angles between θ_r and a maximum angle of flow stability θ_{\max} , as well as the dependence of the angle of repose on pile height for shallow piles less than 20-30 grain diameters in depth.

The transition from flowing to static states suggests that for systems generated in this way, θ_r can be regarded as an analogue for the glass transition temperature T_g , and we characterise the transition by the following properties:

- $P(f)$, the probability distribution of normal forces, develops a plateau in the static state.
- The radial distribution function, $g(r)$ develops a split second peak, and growth of the first peak, indicating compaction and increased short-range ordering.
- The average co-ordination number, z_c , jumps discontinuously. Moreover, the static state that results when motion ceases is not isostatic.

Furthermore, we observe a significant change in the number and nature of interparticle contacts: although a finite fraction of contacts are plastic (at Coulomb yield) for all flowing piles, almost none are plastic when the pile becomes static [13]. The average co-ordination number increases continuously towards four in the flowing state and jumps to well above four for the static packing – four being the theoretical minimal co-ordination number for a network of frictional grains.

We carried out molecular dynamics simulations in 3D on a model system of $N = 8000$ mono-disperse, cohesionless, frictional spheres of diameter d and mass m . The system is spatially periodic in the xy (flow – vorticity)-plane, and is constrained by a rough bottom bed in the z -direction, with a free top surface. The static packing height is about $40d$. Particles interact only on contact through a Hertzian interaction law in the normal and tangential directions to their lines of centers [14,15]. That is, contacting particles i and j positioned at \mathbf{r}_i and \mathbf{r}_j experience a relative normal compression

$$\delta = |\mathbf{r}_{ij} - d|,$$

where $\mathbf{r}_{ij} = \mathbf{r}_i - \mathbf{r}_j$, which results in a force

$$\mathbf{F}_{ij} = \mathbf{F}_n + \mathbf{F}_t. \quad (1)$$

The normal and tangential contact forces are given by

$$\mathbf{F}_n = \sqrt{\delta/d} \left(k_n \delta \mathbf{n}_{ij} - \frac{m}{2} \gamma_n \mathbf{v}_n \right), \quad (2)$$

$$\mathbf{F}_t = \sqrt{\delta/d} \left(-k_t \Delta \mathbf{s}_t - \frac{m}{2} \gamma_t \mathbf{v}_t \right), \quad (3)$$

where $\mathbf{n}_{ij} = \mathbf{r}_{ij}/r_{ij}$, with $r_{ij} = |\mathbf{r}_{ij}|$, \mathbf{v}_n and \mathbf{v}_t are the normal and tangential components of the relative surface velocity, and $k_{n,t}$ and $\gamma_{n,t}$ are elastic and viscoelastic constants respectively. $\Delta \mathbf{s}_t$ is the elastic tangential displacement between spheres, obtained by integrating surface relative velocities during elastic deformation of the contact [16]. The magnitude of $\Delta \mathbf{s}_t$ is truncated as necessary to satisfy a local Coulomb yield criterion $F_t \leq \mu F_n$, where $F_t \equiv |\mathbf{F}_t|$ and $F_n \equiv |\mathbf{F}_n|$, and μ is the local particle friction coefficient.

In the steady state flow regime, changes in the particle friction μ , the damping coefficients $\gamma_{n,t}$, or particle hardness k_n , do not change the qualitative nature of our findings [11]. For the present simulations we set $k_n = 2 \cdot 10^5 mg/d$, $k_t = \frac{2}{7} k_n$, $\gamma_n = 50 \sqrt{g/d}$, $\gamma_t = 0.0$, and $\mu = 0.5$ [17]. We choose a time-step $\delta t = 10^{-4} \tau$, where $\tau = \sqrt{d/g}$.

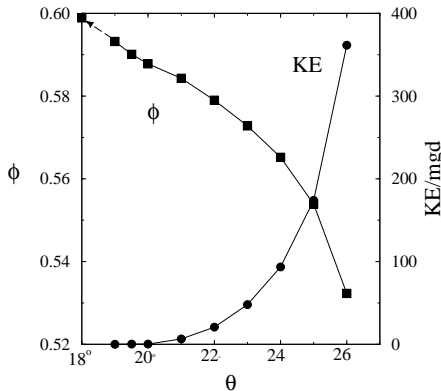


FIG. 1. Bulk packing fraction ϕ and bulk averaged kinetic energy (KE) per particle, normalised by mgd , as a function of tilt angle θ . The dashed arrow indicates the value of ϕ when θ is reduced from 19° to zero.

To initiate flow, we tilt the bed to a large angle ($\theta \approx 26^\circ$) long enough to remove any history effects of construction. We then lower the angle, in unit increments, to the desired value in the range for which there is steady state flow, $20^\circ \lesssim \theta \lesssim 26^\circ$ [10]. In this range, the energy input from gravity is balanced by that dissipated in collisions. We can approach the flowing angles from above and below and always obtain the same results.

Lowering θ , the kinetic energy of the system decreases, however flow continues down to $\theta_r (\simeq 19.4^\circ$ for the set of parameters used here [18]). As θ is reduced, the volume fraction increases, as shown in Fig. 1. We generated further static packings by taking the stopped state at $\theta = 19^\circ$ and reducing the tilt to zero. The volume fraction of the static packing for $\theta = 0.0$, $\phi = 0.599 \pm 0.005$, is less than the random close packing value $\phi_{rcp} \simeq 0.64$.

In order to investigate the distribution of contact forces in flowing and static states, we computed the probability density function (PDF) $P(f)$, where $f \equiv F_n/\bar{F}_n(z)$ is the ratio of the normal contact force magnitude F_n to its average value at the depth z of each contact. Since our system is spatially periodic in the horizontal plane, with no side-walls, the pressure does not saturate with depth, requiring separate averaging at each value of z . The data were averaged over 1000 configurations over a period of 200τ in the steady state at each flowing angle and 5 configurations for the static states.

As shown in Fig. 2, the PDFs exhibit familiar exponential tails at high forces. When θ is reduced towards θ_r , a plateau develops near $f = 1$ (see inset), similar to the behaviour observed in Ref. [8] near the glass transition. It may be argued on this basis that θ_r appears analogous to T_g in a glass-former. However, the development of this feature is rather subtle in our system, and does not appear to be a sharp indicator of the transition from the flowing to the static case. Upon further relaxation of the stress by reducing θ to zero, the feature becomes more prominent similar to the results in Ref. [9].

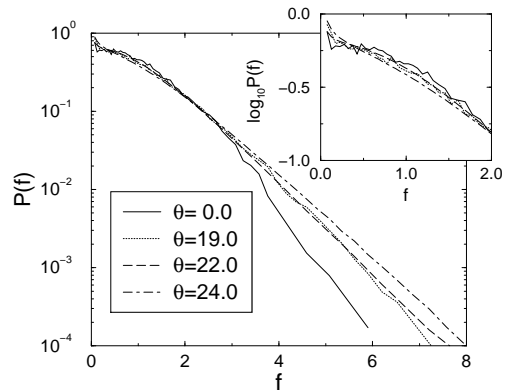


FIG. 2. Distribution of normal contact forces $P(f)$ for various tilt angles (see text). The inset shows the emergence of a plateau in $P(f)$ at small forces for the static systems.

As with glass transitions, we have found only subtle structural evidence for the transition from flow to rest. The radial distribution function $g(r)$ is fairly insensitive to the tilt angle, as shown in Fig. 3. Although there is no long range ordering, in the inset to Fig. 3 we observe the gradual splitting of the second peak as θ is reduced. The system develops more locally ordered structures as it becomes more compact [19].

More significantly, the first peak in $g(r)$ increases with decreasing θ . Because particle neighbors are defined only on contact in our simulations, the first peak in the radial distribution function corresponds to the average coordination number z_c , which correspondingly increases as θ decreases (see Fig. 4).

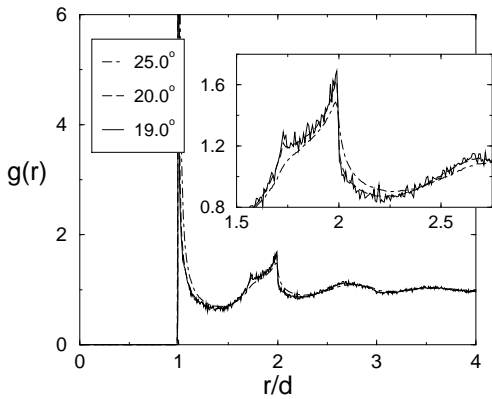


FIG. 3. Radial distribution function $g(r)$ for various tilt angles θ . The inset shows the region near the second peak.

An important characteristic that separates the granular system from a glass forming liquid is the existence of interparticle friction and yield. To explore the influence of intergrain friction, we distinguish between intergrain contacts at their yield criterion $F_t = \mu F_n$ (plastic contacts), which respond plastically to some external perturbations, from contacts with $F_t < \mu F_n$ (elastic contacts), whose response is determined by elastic deformations of the constituent grains. Note that the relationship between plasticity/elasticity of individual contacts between grains and the mechanical response of the entire system has not been explored in this study.

We find that the nature of grain-grain contacts is quite different in the flowing and static regimes. The probability densities of frictional saturations $\zeta \equiv F_t/\mu F_n$ are shown in Fig. 5 for various tilt angles. The fraction n_c of plastic contacts (with $\zeta = 1$) decreases as the tilt angle is decreased towards θ_r (see Fig. 4), accompanied by a decrease in the average frictional saturation of elastic contacts. For the static piles at $\theta < \theta_r$, almost all grain contacts are elastic.

A related question is whether or not static piles of rigid grains satisfy an isostaticity condition, where the number of contacts is the minimum required to satisfy force and torque balance equations for each grain [20]. This isostaticity hypothesis has been frequently invoked in recent theoretical work attempting to derive macroscopic constitutive relations directly from the microstates of static granular packings [21]. Isostaticity is required for a unique determination of the individual contact forces solely in terms of the microstate. Otherwise, the details of grain deformations (for example, Hookean or Hertzian force laws) must be considered in order to determine the stress state of the pile [22], as the rigid grain problem becomes ill-posed.

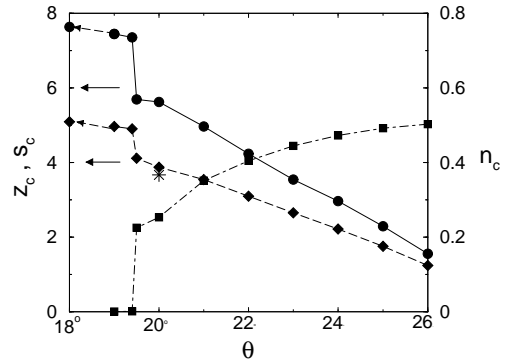


FIG. 4. As the tilt angle is decreased towards θ_r , the fraction of plastic contacts n_c (squares) decreases while the co-ordination number z_c (diamonds) and the staticity index s_c (circles) increase. The isostatic values of z_c and s_c are indicated by the solid arrows. The dashed arrows indicate the values of z_c and s_c when we take θ down to zero from a stopped state. The point indicated by * at $\theta = 20^\circ$ is for $k_n = 2 \cdot 10^7 mg/d$.

Counting the degrees of freedom (DOF) in the contact forces suggests that isostaticity requires $z_c = 4$ for frictional contacts (with 3 DOF - one vector force - per contact and 6 equations per grain) and $z_c = 6$ for frictionless contacts (with 1 DOF - one normal force - per contact but only 3 equations per grain) for spherical grains. However, one DOF is eliminated for each frictional contact that reaches the yield criterion and becomes plastic [22]: the magnitude of the tangential force in this case is determined by the normal force and the friction coefficient μ . Thus, if the fraction of plastic contacts is n_c , for a co-ordination number z_c the total number of DOF characterizing interparticle forces is

$$N_f = \frac{N}{2} z_c [3(1 - n_c) + 2n_c], \quad (4)$$

and requiring $N_f \geq 6N$ to match the number of kinematic constraints on the particles yields

$$s_c \equiv (3 - n_c)z_c/2 \geq 6, \quad (5)$$

where we have defined the staticity index s_c . The equality corresponds to isostaticity. By analogy to the system in Ref. [22], the response of “hyperstatic” piles with $s_c > 6$ to external forces cannot be determined without considering the history of grain contacts.

Figure 4 depicts s_c as a function of θ . As expected, $s_c < 6$ for all flowing piles, though it increases with decreasing θ . However, it appears that a finite jump of s_c at θ_r leaves the static pile significantly hyperstatic. Note however that the point denoted by * in Fig. 4 is for a system where $k_n = 2 \cdot 10^7 mg/d$, indicating that grain hardness is a relevant parameter in determining s_c and z_c [23].

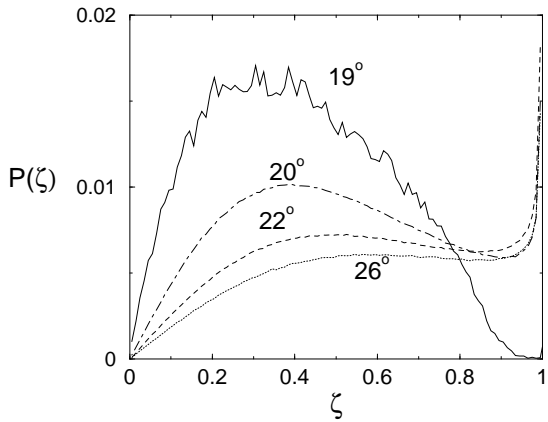


FIG. 5. The probability distribution $P(\zeta)$ of frictional saturation $\zeta \equiv F_t/\mu F_n$ at various tilt angles. In the flowing state a finite fraction of plastic contacts exist (see Fig. 4).

What do these observations teach us about the nature of the “jamming” transition of the granular medium? Our earlier work showed that granular flows obey a local rheology independent of the history of loading [10,11]. Also, static piles are known to generally be able to support a range of external stresses without any macroscopic rearrangement. So, how was the original stress state and associated configuration of grains in this static pile determined? One possible answer is that this state was determined by the local loading conditions at the instant the flow ceased. This resolution is akin to ideas discussed in the fixed principal axes (FPA) model [4], except that the stress state of the static pile, including principal stress axes, do change subsequent to flow arrest (which is manifested as burial in the FPA model) as a function of external loading, due to contact elasticity of grains.

We have observed analogies between jamming of granular media and the glass transition. A plateau in the force distributions appears at small forces once the system ceases to flow, as observed in numerical studies of liquids at the glass transition [8]. Also, more locally ordered structures appear as the system compacts. However, the most significant effect is the transition from a flowing plastic system with a local rheology to a static system that may preserve the fingerprint of the stress state at the instant of jamming, which makes this transition similar to a glass transition, in that glasses also have an ability to be pre-stressed. Finally, we note that we have performed a similar study with Hookean spheres, with essentially the same results.

Sandia is a multiprogram laboratory operated by Sandia Corporation, a Lockheed Martin Company, for the United States Department of Energy under Contract DE-AC04-94AL85000. DL acknowledges support from US-Israel Binational Science Foundation Grant 1999235.

- [1] K. To, P.-Y. Lai, and H. K. Pak, Phys. Rev. Lett. **86**, 71 (2001).
- [2] D. M. Mueth, H. M. Jaeger, and S. R. Nagel, Phys. Rev. E **57**, 3164 (1998).
- [3] M. E. Cates, J. P. Wittmer, J.-P. Bouchaud, and P. Claudin, Phys. Rev. Lett. **81**, 1841 (1998).
- [4] J. P. Wittmer, M. E. Cates, and P. Claudin, J. Phys. I France **7**, 39 (1997).
- [5] R. M. Nedderman, *Statics and Kinematics of Granular Materials* (Cambridge University Press, Cambridge, 1992).
- [6] S. B. Savage, J. Fluid Mech. **92**, 53 (1979).
- [7] A. J. Liu and S. R. Nagel, Nature **396**, 21 (1998).
- [8] C. S. O’Hern, S. A. Langer, A. J. Liu, and S. R. Nagel, Phys. Rev. Lett. **86**, 111 (2001).
- [9] D. L. Blair, N. W. Mueggenburg, A. H. Marshall, H. M. Jaeger, and S. R. Nagel, Phys. Rev. E **63**, 041304 (2001).
- [10] D. Ertas, G. S. Grest, T. C. Halsey, D. Levine, and L. E. Silbert, cond-mat/0005051.
- [11] L. E. Silbert, D. Ertas, G. S. Grest, T. C. Halsey, D. Levine, and S. J. Plimpton, cond-mat/0105071.
- [12] O. Pouliquen, Phys. Fluids **11**, 542 (1999).
- [13] Were we to use a sufficiently large value for interparticle friction, we would not expect plastic contacts even in the flowing state.
- [14] O. R. Walton and R. L. Braun, J. Rheo. **30**, 949 (1986).
- [15] P. A. Cundall and O. D. L. Strack, Géotechnique **29**, 47 (1979).
- [16] We also take into account the rigid body motion around the contact point, ensuring that $\Delta \mathbf{s}_t$ always remains in the local tangent plane of contact.
- [17] Since the coefficient of restitution is dependent on \mathbf{v}_n and goes to 1 as $\mathbf{v}_n \rightarrow 0$, we increased the global damping for $\theta < \theta_r$ after the measured kinetic energy per particle $< 10^{-3} mgd$. This was done to reduce the computer time needed to dissipate the remaining kinetic energy. In the static case the simulations were continued until the average kinetic energy per particle was less than $10^{-8} mgd$.
- [18] In general, the specific values of θ_r and θ_{max} depend on μ and γ_n , and are sensitive to roughness of the fixed bed.
- [19] A. S. Clarke and H. Jonsson, Phys. Rev. E **47**, 3975 (1993).
- [20] C. F. Moukarzel, Phys. Rev. Lett. **81**, 1634 (1998).
- [21] S. F. Edwards and D. V. Grinev, Physica A **263**, 545 (1999).
- [22] T. C. Halsey and D. Ertas, Phys. Rev. Lett. **83**, 5007 (1999).
- [23] L. E. Silbert, D. Ertas, G. S. Grest, T. C. Halsey, and D. Levine, in preparation (unpublished).